

# Improved bioactivity of GUMMETAL<sup>®</sup>, Ti<sub>59</sub>Nb<sub>36</sub>Ta<sub>2</sub>Zr<sub>3</sub>O<sub>0.3</sub>, via formation of nanostructured surfaces

Journal of Tissue Engineering  
Volume 9: 1–8  
© The Author(s) 2018  
Reprints and permissions:  
sagepub.co.uk/journalsPermissions.nav  
DOI: 10.1177/2041731418774178  
journals.sagepub.com/home/tej



Shiva Kamini Divakarla<sup>1,2</sup>, Seiji Yamaguchi<sup>3</sup>, Tadashi Kokubo<sup>3</sup>, Dong-Wook Han<sup>4</sup> , Jae Ho Lee<sup>5,6</sup> and Wojciech Chrzanowski<sup>1,2</sup>

## Abstract

The leading reason for implant revision surgery globally is lack of implant integration with surrounding bone. A new titanium alloy GUMMETAL<sup>®</sup> (Ti<sub>59</sub>Nb<sub>36</sub>Ta<sub>2</sub>Zr<sub>3</sub>O<sub>0.3</sub>) is currently used in biomedical devices and has a Young's modulus that is better matched to bone. The surface was subject to NaOH, CaCl<sub>2</sub>, heat and water treatment (BioGum) after which the surfaces were evaluated using atomic force microscope, scanning electron microscope, X-ray diffractometer and elemental analysis using energy dispersive X-ray. To demonstrate enhanced bone bonding ability and cytocompatibility, apatite formation in simulated body fluid and *in vitro* stem cell attachment, proliferation and cytoskeleton organisation were examined. The formation of a ~200 nm nanoscale needle-like calcium titanate network on the surface following treatment was revealed and upon soaking in simulated body fluid, the formation of a ~5 μm layer of apatite. Metabolic activity of rat bone marrow stem cells on BioGum was increased in comparison to control and the cell number appeared greater, with more elongated morphology as early as 2 h post-seeding. This positions the modification as a simple and potentially universal technology for the improvement of implant integration.

## Keywords

Implant integration, bioactivity, atomic force microscopy, biocompatibility, titanium implants, orthopaedic implants

Date received: 2 March 2018; accepted: 9 April 2018

## Background

More than 1 million total joint replacement surgeries occur annually in countries that are part of the Organisation for Economic Co-operation and Development (OECD) and this number has been steadily increasing; the number of hip replacements performed increased by 35% and the number of knee replacements doubled between 2000 and 2013.<sup>1</sup> The leading reason for implant revision surgery globally is aseptic loosening or lack of integration of the implant to the surrounding bone.<sup>2</sup> Integration of implants can occur via two main mechanisms, either indirectly through a fibrous tissue layer at the bone-implant surface (fibro-osseous integration), or by the growth of bone directly on the implant surface (osseointegration).<sup>3</sup> The former is undesirable, especially in load-bearing implants due to the loosening of implants and subsequent functional failure of the device, while osseointegration represents more rigid fixation of a foreign material within an osseous

tissue, maintained during functional loading. A contiguous material-bone interface occurs when osteogenic and stem

<sup>1</sup>Faculty of Pharmacy, The University of Sydney, Sydney, NSW, Australia

<sup>2</sup>The University of Sydney Nano Institute, Sydney, NSW, Australia

<sup>3</sup>Department of Biomedical Sciences, College of Life and Health Sciences, Chubu University, Kasugai, Japan

<sup>4</sup>Department of Cogno-Mechatronics Engineering, College of Nanoscience & Nanotechnology, Pusan National University, Busan, Korea

<sup>5</sup>CHA Fertility Center, Seoul Station, Seoul, Republic of Korea

<sup>6</sup>Department of Biomedical Science, College of Life Science, CHA University, Pochon, Republic of Korea

## Corresponding author:

Shiva Kamini Divakarla, The University of Sydney Nano Institute, Sydney, NSW 2006, Australia.

Email: shiva.divakarla@sydney.edu.au



cells are recruited to the injury site, attach, proliferate and differentiate. Recent evidence shows that this recruitment is coordinated by an active release of chemoattractants, that is, extracellular vesicles (EVs), by resident cells at the injury site. Furthermore, EVs have been shown to have the potential to promote cell differentiation.<sup>4</sup> Since EV release and composition are stimulated by the environment including surface, it is hypothesised that modification of the surface characteristics activates production of EVs that are capable to trigger differentiation of recipient cells.<sup>4</sup> However, EVs are heterogenous in nature and can package different molecular cargo, which may result in nonspecific cell 'programming'. Recent advances in this area have demonstrated that heterogeneity of EVs can be assessed in high resolution and specific populations of EV can be identified and sorted to achieve the desired cell modulation. In summary, cell differentiation is orchestrated by the environmental factors including topography and surface chemistry as well as biological signals packaged in EVs 'manufactured' actively by cells, which is coordinated by environmental cues such as surface topography and chemistry.<sup>5</sup> Consequently, through these stimulations, cells deposit collagenous bone matrix directly on the surface, which is then rapidly mineralised, forming a robust connection between implant and tissues.

Load-bearing orthopaedic implants are composed of three main classes of materials: metals, ceramics and polymers. Metals remain a dominant group due to their high mechanical properties. A significant proportion of metallic implants, including bone fixation devices, spinal implants and knee and hip endoprostheses are made of titanium alloys such as Ti6Al4V and Ti6Al7Nb.<sup>6</sup> The elastic modulus of traditional titanium alloys is several orders of magnitude greater than human bone and this may lead to implant loosening due to stress shielding, which is bone resorption due to higher load or stress.<sup>7</sup> A new titanium alloy, GUMMETAL<sup>®</sup>-Ti<sub>59</sub>Nb<sub>36</sub>Ta<sub>2</sub>Zr<sub>3</sub>O<sub>0.3</sub>, has recently been developed and used in biomedical devices.<sup>7</sup> GUMMETAL's Young's modulus (40 GPa) is better matched to bone (which lies between 10 and 30 GPa in comparison to commercially pure titanium (100–110 GPa<sup>8</sup>) and other commonly used implant metals, such as stainless steel (around 200 GPa<sup>9</sup>), minimising the stress shielding phenomenon. It has a higher strength than traditional alloys (>1000 MPa) and does not incorporate carcinogenic elements such as Al and V. This alloy, introduced by Toyota Tsusho Corp, Japan is now used by Kyocera Medical Corp, and was recently described in patents for bone implants held by Synthes.<sup>10</sup> It has been commercialised for some orthopaedic implants including plates, screws, dental implants and so on. However, bare titanium alloy surfaces fail to effectively stimulate cell attachment and growth.<sup>11,12</sup> Sub-optimal mechanical properties and the limited osteoinductivity therefore necessitates the search for both new types of alloys with lower elastic modulus

and effective methods of surface modification to enable their osseointegration.<sup>13</sup>

Various forms of surface modification of metal substrates have been suggested, including nano- and micro-topographical modification, hydroxyapatite (HA) spray coating, electrochemical treatments and ion implantation methods.<sup>14–17</sup> Among the major limitations of these treatments is the inability to treat implants with complex geometries, very high cost and a need for advanced facilities. Chemothermal treatments have also been suggested to modify the surface and are advantageous due to the lack of expensive apparatus required for modification.<sup>7,18</sup> In this study, we developed simple NaOH, CaCl<sub>2</sub>, heat and water treatment of GUMMETAL (Ti<sub>59</sub>Nb<sub>36</sub>Ta<sub>2</sub>Zr<sub>3</sub>O<sub>0.3</sub>) surface to promote bone-bonding ability. This strategy for proactive implant osseointegration characterises with: (1) robust bioactive interface that resists delamination as being built from the surface, (2) incorporates key ions to promote the formation of the apatite like structure directly on the surface and (3) nanostructured and highly cell-adhesive surface to encourage cell colonisation.

The presented strategy integrates key strengths on new titanium alloys with superior mechanical properties and cost-effective treatment that impart bone bonding ability. These advances that aim to minimise adverse reactions through improved implant properties and integration within the body are of great significance. Since there has been a steady increase in implant numbers and statistical data suggest that implant applications will skyrocket over the next few decades, the proposed innovation has great promise to provide multifunctional surfaces that improve osseointegration of orthopaedic implants.

## Materials and methods

### Surface treatments

The Ti–36Nb–2Ta–3Zr–0.3O alloy sheet (GUMMETAL<sup>®</sup>; Toyota Central Research and Development Laboratories, Inc., Japan, Ti: 58.43, Nb: 36.39, Ta: 2.00, Zr: 2.87, O: 0.31, Fe: 0.02 mass%) was cut into rectangular plates which were 10 × 10 × 1 mm in size, abraded with #400 diamond plates, and washed with acetone, 2-propanol and ultrapure water in an ultrasonic cleaner for 30 min each and dried at 40°C. The surface modification was done in a few steps:

1. Chemical treatment I: (a) soaking in 5 mL of a 1 M NaOH aqueous solution (Nacalai Tesque Inc., Kyoto, Japan) at 60°C for 24 h. After removal from the solution, they were gently rinsed with ultrapure water for 30 s and dried at 40°C and (b) soaking in 10 mL of 100 mM CaCl<sub>2</sub> solution at 40°C for 24 h, and washed with ultrapure water and dried.
2. Heat treatment: samples were heated up to 700°C at a rate of 5°C min, kept for 1 h at the respective

temperature in an ambient atmosphere and this was followed by natural cooling in an electrical furnace.

3. Water treatment: soaking in 10 mL of ultrapure water at 80°C for 24 h, then washed and dried.

Next, samples subjected to the chemical and heat treatments were soaked in 24 mL of simulated body fluid (SBF) at various ion concentrations ( $\text{Na}^+$  142.0,  $\text{K}^+$  5.0,  $\text{Ca}^{2+}$  2.5,  $\text{Mg}^{2+}$  1.5,  $\text{Cl}^-$  147.8,  $\text{HCO}_3^-$  4.2,  $\text{HPO}_4^{2-}$  1.0 and  $\text{SO}_4$  0.5 mM) nearly equal to those of human blood plasma at 36.5°C. The SBF was prepared by dissolving reagent grade NaCl,  $\text{NaHCO}_3$ , KCl,  $\text{K}_2\text{HPO}_4 \cdot 3\text{H}_2\text{O}$ ,  $\text{MgCl}_2 \cdot 6\text{H}_2\text{O}$ ,  $\text{CaCl}_2$  and  $\text{Na}_2\text{SO}_4$  (Nacalai Tesque Inc., Kyoto, Japan) in ultrapure water and buffered at pH=7.4 with tris(hydroxymethyl) aminomethane  $(\text{CH}_2\text{OH})_3\text{CNH}_2$  and 1 M HCl (Nacalai Tesque Inc., Kyoto, Japan) at 36.5°C. After soaking in the SBF for 7 days, the samples were gently rinsed with ultrapure water and dried.

## Surface characterisation

### Analysis of the surface morphology

**Scanning electron microscopy.** The surfaces and cross-sections of the metal samples untreated, Ca-treated and subsequently soaked in SBF were coated with a Pt–Pd thin film and observed under a field emission scanning electron microscope (FE-SEM: S-4300, Hitachi Co., Tokyo, Japan) at a voltage of 15 kV.

**Atomic force microscopy.** The topography of GUM-METAL samples were analysed using atomic force microscope (AFM) (Park, XE-70, Korea). The samples were scanned in non-contact mode using ACTA cantilever (Olympus). Two sizes of images were recorded at  $45 \mu\text{m} \times 45 \mu\text{m}$  and  $10 \mu\text{m} \times 10 \mu\text{m}$ . Images were processed using SPIP software (Image Metrology A/S, Denmark); roughness parameters ( $R_a$ ) were obtained from both the scan sizes.

### Analysis of the surface structure

**Thin-film X-ray diffraction.** Surfaces were analysed using a thin-film X-ray diffractometer (TF-XRD; model RNT-2500, Rigaku Co., Japan). TF-XRD was performed using a CuK $\alpha$  X-ray source operating at 50 kV and 200 mA. The glancing angle of the incident beam was set to an angle of 1° against the sample surface.

### Analysis of the surface chemistry

**Elemental analysis; energy dispersive X-ray analysis.** The surface chemical composition of the metal samples untreated, Ca-treated, and subsequently soaked in SBF was analysed by an energy dispersive X-ray (EDX) spectrometer (EDX: EMAX-7000, Horiba Ltd., Kyoto, Japan) at 9 kV–K for C, O, Ti, Nb, Ta, Zr, P, Ca, Mg and Na five areas, and their averaged value was used for analysis.

## In vitro cell responses

**Cell adhesion.** To investigate the influence of the surface modifications on cell attachment, rat bone marrow stem cells (rMSCs) were cultured on the materials for 2 and 5 h. The attachment was evaluated by counting the total number of cells on 10 confocal images acquired from different locations of the samples. Counted cell numbers were related to the surface area of the images and presented as the cell density that represents cell attachment. The isolation of rMSCs and their culture methods are fully described in our previous work<sup>19</sup> and the experiments are approved by the Animal Care and Use Committee of Dankook University.

Cells were suspended and cultured under a normal culture medium containing minimal essential medium ( $\alpha$ -MEM) plus 1% antibiotic/antimycotic and 10% foetal bovine serum in a humidified atmosphere of 5%  $\text{CO}_2$  at 37°C. Adherent cells were expanded and sub-cultured for 2–3 passages for further use. Sub-cultured rMSCs were harvested and seeded at  $1 \times 10^5$  cell/mL on each sample and then cultured for 2 and 5 h. Cell nuclei, focal adhesion kinase (FAK) and F-actin were stained (Alexa Fluor 488 Phalloidin, ThermoFisher) and the images were captured using a confocal scanning microscope (Nikon C2, Japan). The DAPI-positive cells counted from different image fields are taken as the number of cells adhered to the sample.<sup>20</sup>

**Metabolic activity.** The metabolic activity of cells was measured using the PrestoBlue™ assay (ThermoFisher, USA). In all, 25  $\mu\text{L}$  (10% of medium volume) of PrestoBlue dye was added to each well and the plates were incubated for a period of 2 h. The fluorescent activity of the extracted aliquot was then measured using fluorescent plate reader (Fluoroskan Ascent plate reader, type 374, Labsystems, Finland.) Readings were performed after 24 h (day 1), 72 h (day 3), 168 h (day 7) and 336 h (day 14). Statistical analysis of measurements was completed using two-way analysis of variance (ANOVA) and Sidak's multiple comparisons test using the programme GraphPad Prism 7.02.

## Results and Discussion

### Surface characterisation

#### Analysis of the surface morphology

**SEM.** Figure 1(a) depicts SEM images of the untreated GUMMETAL® surface. The surface modification (heat and alkali treatment) resulted in the formation of a nanoscale needle-like network structure on the surface (Figure 1(b)). Nanostructured surfaces which presented similar morphology were previously shown to promote integration of the material with tissues.<sup>21,22</sup> The cross-sectional image confirmed that the layer thickness was ~200 nm and the layer

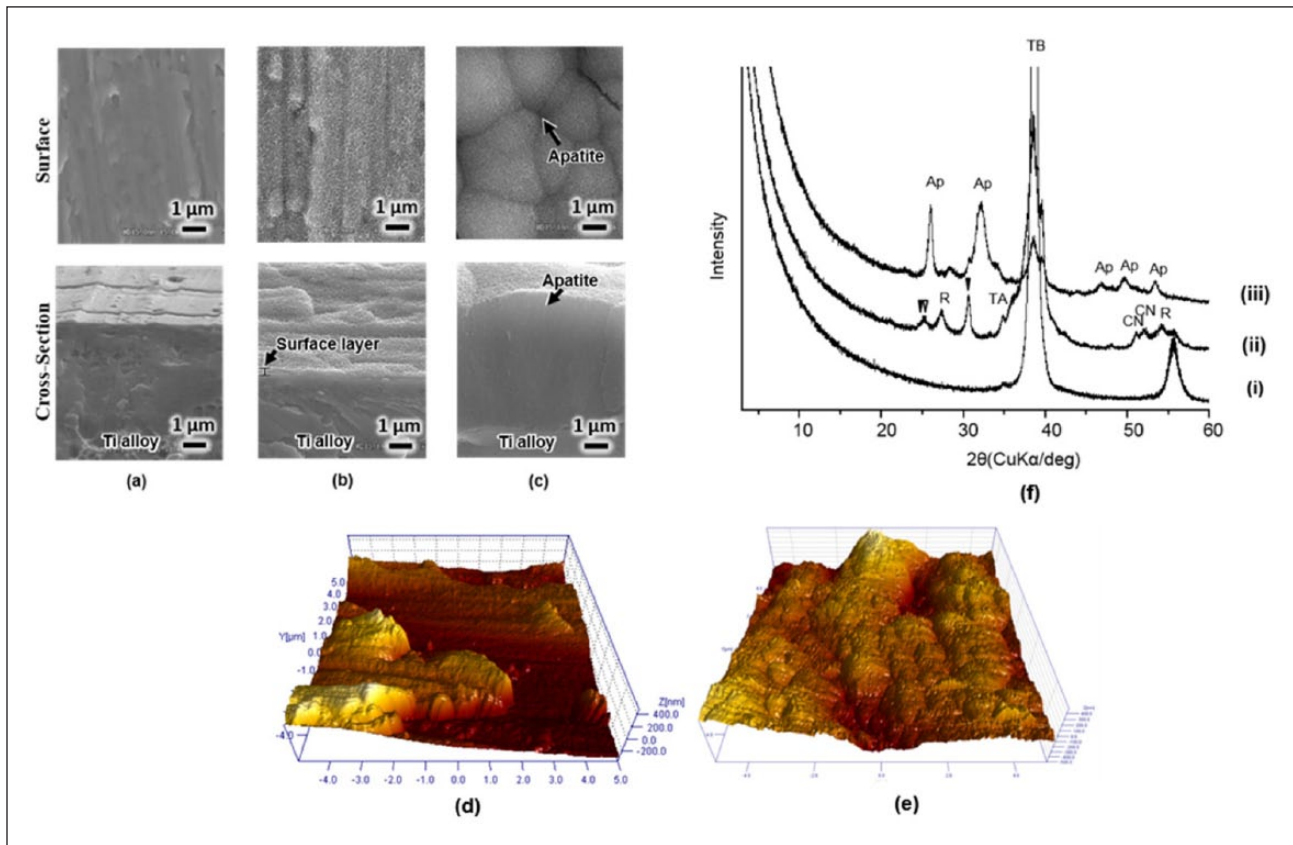


**Figure 1.** FE-SEM images of the surfaces and cross-sections of GUMMETAL® (a) untreated, (b) subjected to NaOH, CaCl<sub>2</sub>, heat and water treatment (BioGum) and (c) subsequently soaked in SBF for 7 days. AFM images of (d) Ti-36Nb-2Ta-3Zr-0.3O alloy untreated and (e) NaOH, CaCl<sub>2</sub>, heat and water treated surfaces. TF-XRD profiles of (f) surfaces of Ti-36Nb-2Ta-3Zr-0.3O alloy: (i) untreated, (ii) subjected to NaOH, CaCl<sub>2</sub>, heat and water treatment and (iii) subsequently soaked in SBF for 7 days.

was very uniform. The deposition of HA from SBF on the modified surfaces, is made apparent through the globular layer in Figure 1(c), while the cross-sectional image displays the apatite layer thickness to be  $\sim 5 \mu\text{m}$ . It is well understood that Ti-based alloys with surfaces conducive to apatite formation in SBF possess greater bone-bonding ability as the SBF mimics the ionic composition of human plasma.<sup>23</sup> This suggests that surface modification significantly improved the rate of the apatite deposition, which consequently suggests the improvement in osseointegration.

**AFM.** Changes in surface morphology are evident via visual and quantitative analysis of AFM image following surface modification. The rough edges of the control sample produced by abrasion (Figure 1(d)) were visibly smoother following the modification (Figure 1(e)). The average surface roughness ( $S_a$ ) increased at the  $45 \mu\text{m}$  scan size from  $486 \text{ nm}$  to  $573 \text{ nm}$ .

Previous studies have shown that modification of surface roughness through ‘engraving’ specific features onto the surface (as observed here) promotes HA formation in SBF and the promotion of osteoblast adhesion and differentiation.<sup>24,25</sup> Changes in surface roughness also

correspond to increased formation of the HA layer, highlighting the potential of the material for bone implants. However, promotion of the HA formation was rather attributed to chemical composition of the surface after the chemical treatments. The treatment was designed to enrich the surface in Ca ions which are effectively exchanged with  $\text{H}_3\text{O}^+$  ions when the material is in contact with SBF. The active ion exchange results in accelerate formation of the apatite, which in turn correlates with potential improved integration with bone tissues.<sup>20</sup>

### Analysis of the surface structure

**Thin-film X-ray diffraction.** XRD analysis confirmed the formation of rutile (denoted by ‘R’), calcium niobate and calcium titanate (indicated by the ‘CN’ and downward arrows, respectively) on the surface after the treatment (Figure 1(f(ii))). This further supports that there is formation of an amorphous sodium titanate and niobate layer formed following treatment with NaOH, which is then converted into the aforementioned crystalline Ca compounds following heat and water treatment.<sup>26</sup> However, the alkali-heat treatment alone did not promote apatite formation in SBF as seen



**Table 1.** EDX results of surface layers of untreated GUMMETAL® and GUMMETAL® subjected to NaOH, CaCl<sub>2</sub>, heat and water treatments (Biogum) and subsequently soaked in SBF for 7 days.

Treatment	Elements/at%									
	C	O	Ti	Nb	Ta	Zr	P	Ca	Mg	Na
Untreated	2.7	11.3	61.3	22.5	0.6	1.6	0	0	0	0
NaOH-CaCl <sub>2</sub> -heat-water	4.1	65.1	19.9	7.5	0.2	0.6	0	2.7	0	0
NaOH-CaCl <sub>2</sub> -heat-water-SBF	7.2	61.9	0	0	0	0	12.1	17.8	0.6	0.3

EDX: energy dispersive X-ray; SBF: simulated body fluid.

with other titanium alloy (Ti-Zr-Nb-Ta) due to the slow release of calcium ions from the calcium titanates and niobates. The water treatment step appears to be essential in promoting apatite formation through its ability to mobilise the Ca<sup>2+</sup> ions, hence forming a ‘bioactive’ interface for apatite formation.<sup>27</sup> The formation of apatite on the alkali-CaCl<sub>2</sub>-heat-water treated surface soaked in SBF was confirmed using XRD (Figure 1(f(iii))).

### Analysis of the surface chemistry

**EDX analysis.** EDX analysis (Table 1) showed reduction in Ti%, Nb%, Ta%, Zr% and the dramatic increase of O on the surface following alkali-heat treatment, which confirms the formation of an interface on the original untreated surface. Furthermore, the presence of Ca (2.7 atm%) following NaOH-CaCl<sub>2</sub> and heat-water treatment but not Na suggests the exchange of Na and Ca ions on the surface. This change in the surface chemistry implies that the ‘bioactive’ interface has been created on the GUMMETAL. The further increase in Ca (2.7%–17.8 atm%) and the presence of P at 12.1 atm% following soaking in SBF confirmed calcium phosphates were rapidly formed on the modified samples, as well as the presence of trace amounts of Na and Mg (which are similar to bone mineral<sup>28</sup>) indicate the high activity of the samples to induce apatite layer formation, ultimately enhancing bone bonding ability.<sup>23</sup> The Ca/P ratio was calculated to be 1.47, which suggests the formation of crystalline apatite on the surface. This occurrence is due to the exchange of surface Na<sup>+</sup> with the Ca<sup>2+</sup> ions from the CaCl<sub>2</sub>, followed by rapid formation of an amorphous calcium titanate layer. Following this, more Ca ions from SBF are able to bond to the surface and with further soaking in SBF, the Ca<sup>2+</sup> ions accumulate, allowing for negatively charged phosphate ions to develop amorphous calcium phosphate on the surface, which is then converted to crystalline apatite.<sup>22,29</sup> The lack of detection of Ti, Nb, Ta, Zr following soaking in SBF is also in agreement with the SEM images which display the thick layer of apatite formed on the surface.

### In vitro cell responses

**Adhesion and metabolic activity of rMSCs.** Metabolic activity of the rMSCs was established through the PrestoBlue

assay. Cell metabolism remained similar between the control and treated sample days 1–7, after which at day 14, it was significantly higher on the BioGum surface in comparison to the untreated surface (Figure 2(b)). The cell density on the BioGum surface was also greater at each time point, evident through the DAPI stain and the formation of well-developed (stretched) actin filament network and focal adhesions, suggesting that the apatite layer promotes cell attachment. The unfavourable spherical shape of the cells on the control sample at the 2 h time point suggests poor adhesion, in comparison to the visually stretched and well-adhered cells on the GUMMETAL® sample.<sup>30</sup> While the cells adhered on the untreated GUMMETAL® sample also appeared stretched at later time points (Figure 2(a)), this was more likely attributed to cells orienting themselves on grooves established by the initial abrasion. Focal adhesion density was greater on treated samples in comparison to the untreated sample. This suggests the cells are able to effectively ‘anchor’ themselves to a greater degree on the BioGum surface. Cytoskeletons of cells cultured on Biogum samples were well organised with actin microfilaments radiating in all directions (Figure 2(a), increased appearance at higher magnification in Figure 2(d)), in comparison with the untreated surface (Figure 2(a) and (c)).

The initial adhesion of mesenchymal stem cells on the biomaterial surface is an important determinant of cell survival, proliferation and differentiation. Therefore, initial cell adhesion and morphology regulate focal adhesion proteins such as FAK. Focal adhesion protein is also linked with actin-cytoskeleton formation for regulation of favourable cell behaviour.<sup>31</sup>

Previous results suggest that surface modifications of titanium using NaOH and thermal treatment, lead to the formation of specific, cell stimulating nanostructures<sup>32,33</sup> and change chemical composition at the interface.<sup>34</sup> These changes cumulatively promote more favourable cell adhesion with well developed FAK.<sup>20,35</sup> Consequently, upregulated expression of alkaline phosphatase, a marker of osteoblastic differentiation (which is correlated with increased calcium phosphate formation in SBF and bone-tissue integration<sup>27</sup>), was observed when two subtypes of cells were used: rat calvarial cells<sup>20</sup> and rat bone marrow cells.<sup>36</sup> Given the additional stabilisation of the calcium titanate layer and subsequent improvement in the formation

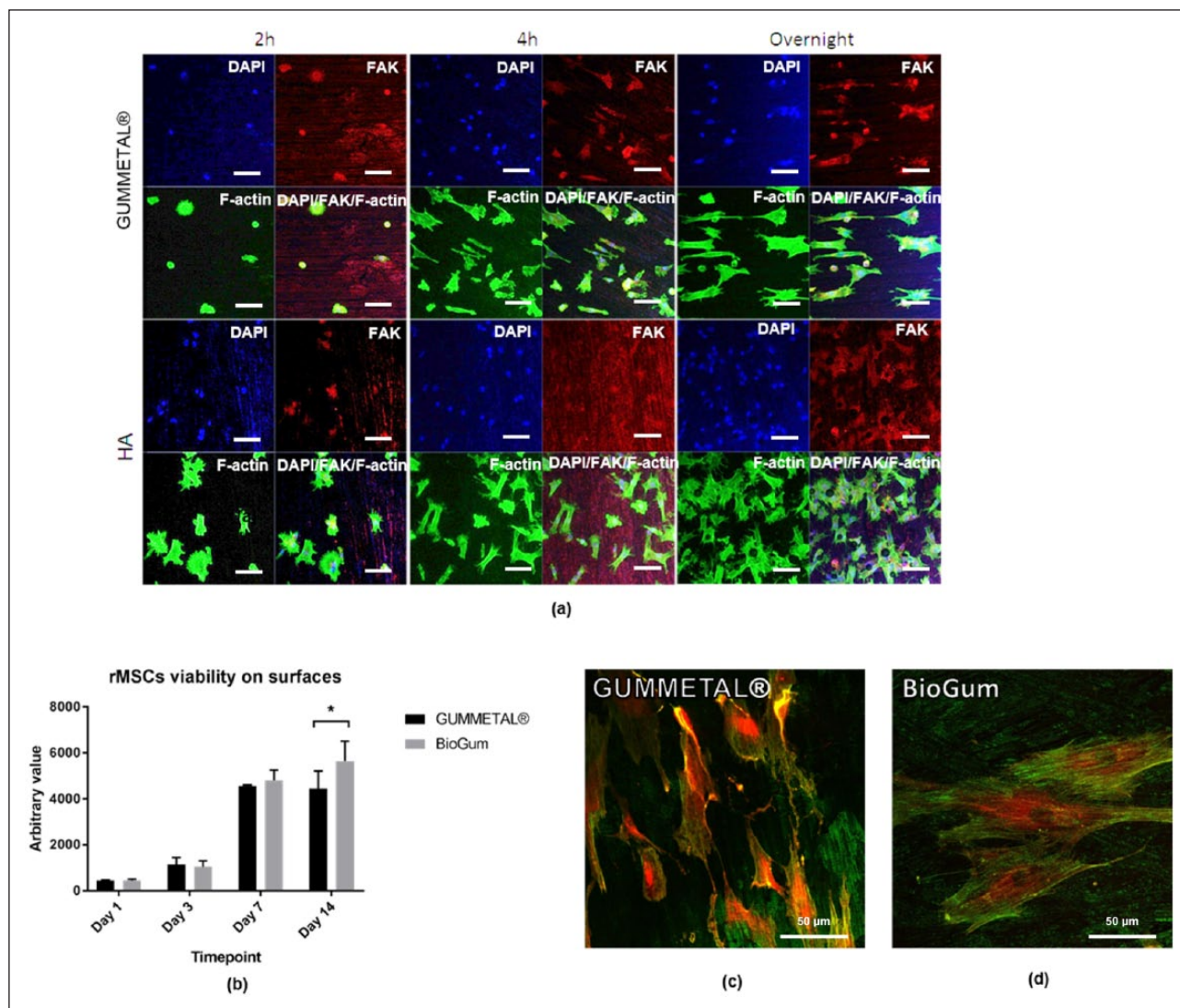


**Figure 2.** (a) Metal surface mesenchymal stem cell adhesion assay for control sample (top row) and hydroxyapatite sample (bottom row). For each individual set of four images – from top left to right: DAPI (blue), focal adhesion kinase stain (red), bottom left to right: F-actin (green) and all three results merged as labelled; scale bar 100 μm. (b) PrestoBlue assay for GUMMETAL®, with (\*) indicating statistical significance ( $p < 0.05$ ) and BioGum and immunostaining of stem cells grown on GUMMETAL® samples, after 24h in culture for (c) GUMMETAL® and (d) BioGum.

of apatite in this study, it could be expected that this treatment regimen on titanium surfaces could similarly (or to a greater degree) promote bone-tissue integration *in vivo*.

## Conclusion

Along with improving life expectancy (up from 49.2 years a century ago to over 78 years now), trauma too has significantly increased demand for orthopaedic implants. In contrast to previous attempts to modify orthopaedic implants, our biomimicry strategy delivers the bi-functionality of matching stiffness of material to the bone and bioactivity of the surface. We demonstrated that surface modification that combines nanostructuring and incorporation of key ions that drive apatite layer formation improved cell

adhesion and proliferation. Since it is well established that both aspects are required to induce cell differentiation and mineralisation, we can anticipate that implants modified using this strategy may achieve the desired fusion with the surrounding bone. A significant competitive advantage of our approach is that NaOH, CaCl<sub>2</sub>, heat and water treatment is an inexpensive and simple method for modification of the surface morphology and chemistry. Based on the results of physicochemical characterisation and *in vitro* stem cell responses, we conclude that surface modification of Ti<sub>59</sub>Nb<sub>36</sub>Ta<sub>2</sub>Zr<sub>3</sub>O<sub>0.3</sub> improves apatite formation on the surface through ion exchange, which forms a ‘bioactive’ layer on the surface. Furthermore, we conclude that the methodology we adopted is effective in promoting cell adhesion and proliferation, thus enhancing ‘bioactivity’ of

GUMMETAL<sup>®</sup>. Hence, this technique could potentially be adopted as a universal strategy for the simple and effective surface modification of existing titanium-based implant materials.

### Declaration of conflicting interests

The author(s) declared no potential conflicts of interest with respect to the research, authorship, and/or publication of this article.

### Funding

The author(s) received no financial support for the research, authorship, and/or publication of this article.

### ORCID iDs

Dong-Wook Han  <https://orcid.org/0000-0001-8314-1981>

### References

1. OECD. *Health at a Glance 2015*. Paris: OECD Publishing, 2015.
2. Sadoghi P, Liebensteiner M, Agreiter M, et al. Revision surgery after total joint arthroplasty: a complication-based analysis using worldwide arthroplasty registers. *J Arthroplasty* 2013; 28: 1329–1332.
3. Parithimarkalaignan S and Padmanabhan TV. Osseointegration: an update. *J Indian Prosthodont Soc* 2013; 13: 2–6.
4. Bjorge IM, Kim SY, Mano JF, et al. Extracellular vesicles, exosomes and shedding vesicles in regenerative medicine – a new paradigm for tissue repair. *Biomater Sci* 2018; 6: 60–78.
5. Kim SY, Khanal D, Tharkar P, et al. None of us is the same as all of us: resolving heterogeneity of stem cell-derived extracellular vesicles using single-vesicle, nanoscale characterization with high-resolution resonance enhanced atomic force microscope infrared spectroscopy (AFM-IR). *Nanoscale Horiz*. Epub ahead of print 1 March 2018. DOI: 10.1039/C8NH00048D.
6. Saini M, Singh Y, Arora P, et al. Implant biomaterials: a comprehensive review. *World J Clin Cases* 2015; 3: 52–57.
7. Tanaka M, Takemoto M, Fujibayashi S, et al. Bone bonding ability of a chemically and thermally treated low elastic modulus Ti alloy: gum metal. *J Mater Sci Mater Med* 2014; 25: 635–643.
8. Black J and Hastings G. Titanium and titanium alloys. In: Black J and Hastings G (eds) *Handbook of biomaterial properties*. Boston, MA: Springer, 1998, pp. 179–200.
9. Niinomi M, Liu Y, Nakai M, et al. Biomedical titanium alloys with Young's moduli close to that of cortical bone. *Regen Biomater* 2016; 3: 173–185.
10. Ahmed T and Rack HJ. Low modulus biocompatible titanium base alloys for medical devices. US5871595A Patent, USA, 1999.
11. Chrzanowski W, Abou Neel EA, Armitage DA, et al. Surface preparation of bioactive Ni-Ti alloy using alkali, thermal treatments and spark oxidation. *J Mater Sci Mater Med* 2008; 19: 1553–1557.
12. Chrzanowski W, Neel EAA, Armitage DA, et al. Effect of surface treatment on the bioactivity of nickel–titanium. *Acta Biomater* 2008; 4: 1969–1984.
13. Liu X, Chu PK and Ding C. Surface modification of titanium, titanium alloys, and related materials for biomedical applications. *Mater Sci Eng* 2004; 47: 49–121.
14. Aparicio C, Padros A and Gil FJ. In vivo evaluation of micro-rough and bioactive titanium dental implants using histometry and pull-out tests. *J Mech Behav Biomed Mater* 2011; 4: 1672–1682.
15. Filiz S, Xie L, Weiss LE, et al. Micromilling of microbarbs for medical implants. *Int J Mach Tool Manu* 2008; 48: 459–472.
16. Karazisis D, Ballo AM, Petronis S, et al. The role of well-defined nanotopography of titanium implants on osseointegration: cellular and molecular events in vivo. *Int J Nanomedicine* 2016; 11: 1367–1382.
17. Pham MT, Matz W, Grambole D, et al. Solution deposition of hydroxyapatite on titanium pretreated with a sodium ion implantation. *J Biomed Mater Res* 2002; 59: 716–724.
18. Nishiguchi S, Fujibayashi S, Kim H-M, et al. Biology of alkali- and heat-treated titanium implants. *J Biomed Mater Res A* 2003; 67: 26–35.
19. Chrzanowski W, Lee JH, Kondyurin A, et al. Nano-biochemical braille for cells: the regulation of stem cell responses using Bi-functional surfaces. *Adv Funct Mater* 2015; 25: 193–205.
20. Chrzanowski W, Kondyurin A, Lee JH, et al. Biointerface: protein enhanced stem cells binding to implant surface. *J Mater Sci Mater Med* 2012; 23: 2203–2215.
21. An S-H, Matsumoto T, Miyajima H, et al. Surface characterization of alkali- and heat-treated Ti with or without prior acid etching. *Appl Surf Sci* 2012; 258: 4377–4382.
22. Takadama H, Kim H-M, Kokubo T, et al. TEM-EDX study of mechanism of bonelike apatite formation on bioactive titanium metal in simulated body fluid. *J Biomed Mater Res* 2001; 57: 441–448.
23. Chrzanowski W, Yeow WJ, Rohanzadeh R, et al. Bone bonding ability – how to measure it? *RSC Adv* 2012; 2: 9214–9223.
24. Lai M, Cai K, Hu Y, et al. Construction of microenvironment onto titanium substrates to regulate the osteoblastic differentiation of bone marrow stromal cells in vitro and osteogenesis in vivo. *J Biomed Mater Res A* 2013; 101A: 653–666.
25. Matsuzaka K, Walboomers XF, Yoshinari M, et al. The attachment and growth behavior of osteoblast-like cells on microtextured surfaces. *Biomaterials* 2003; 24: 2711–2719.
26. Fukuda A, Takemoto M, Saito T, et al. Bone bonding bioactivity of Ti metal and Ti-Zr-Nb-Ta alloys with Ca ions incorporated on their surfaces by simple chemical and heat treatments. *Acta Biomater* 2011; 7: 1379–1386.
27. Kokubo T and Yamaguchi S. Growth of novel ceramic layers on metals via chemical and heat treatments for inducing various biological functions. *Front Bioeng Biotechnol* 2015; 3: 176.
28. Kokubo T, Matsushita T, Takadama H, et al. Development of bioactive materials based on surface chemistry. *J Eur Ceram Soc* 2009; 29: 1267–1274.
29. Hamouda IM, Enan ET, Al-Wakeel EE, et al. Alkali and heat treatment of titanium implant material for bioactivity. *Int J Oral Maxillofac Implants* 2012; 27: 776–784.
30. Eisenbarth E, Meyle J, Nachtigall W, et al. Influence of the surface structure of titanium materials on the adhesion of fibroblasts. *Biomaterials* 1996; 17: 1399–1403.



31. Anderson HJ, Sahoo JK, Ulijn RV, et al. Mesenchymal stem cell fate: applying biomaterials for control of stem cell behavior. *Front Bioeng Biotechnol* 2016; 4: 38.
32. McNamara LE, McMurray RJ, Biggs MJP, et al. Nanotopographical control of stem cell differentiation. *J Tissue Eng* 2010; 1: 120623.
33. Chrzanowski W, Szade J, Hart A, et al. Biocompatible, smooth, plasma-treated nickel-titanium surface—an adequate platform for cell growth. *J Biomater Appl* 2012; 26: 707–731.
34. Yamaguchi S, Nath S, Sugawara Y, et al. Two-in-one biointerfaces-antimicrobial and bioactive nanoporous gallium titanate layers for titanium implants. *Nanomaterials* 2017; 7: 229.
35. Gordin DM, Ion R, Vasilescu C, et al. Potentiality of the ‘Gum Metal’ titanium-based alloy for biomedical applications. *Mater Sci Eng* 2014; 44: 362–370.
36. Nishio K, Neo M, Akiyama H, et al. The effect of alkali- and heat-treated titanium and apatite-formed titanium on osteoblastic differentiation of bone marrow cells. *J Biomed Mater Res* 2000; 52: 652–661.

## Appendix I

### Graphical Abstract

